

Characterization of Ti-35Nb alloy surface modified by controlled chemical oxidation for surgical implant applications

Rodrigo Sacramento da Silva¹, Alexandre Antunes Ribeiro¹

¹Instituto Nacional de Tecnologia - INT - Av. Venezuela, 82/Sala 602, Saúde, CEP: 20081-312, Rio de Janeiro, RJ, Brasil.

e-mail: rodrigo.sacramento@int.gov.br, alexandre.antunes@int.gov.br

ABSTRACT

Titanium-Niobium alloys have been studied for biomedical applications due to their satisfactory biocompatibility. In order to improve the long-term implantation, surface modification techniques have been developed to generate suitable topography, roughness, chemical composition, surface energy, etc. Considering this approach, the present work aimed to characterize Titanium-35Niobium (Ti-35Nb) surface modified by controlled chemical oxidation. Ti-35Nb (wt%) substrates were processed by powder metallurgy. The powders were mechanically mixed, uniaxially cold pressed and sintering at 1300°C/2h. Then, the sintered substrates were immersed in a solution consisting of equal volumes of concentrated H₂SO₄ and 30% aqueous H₂O₂ for 4 hours at room temperature under continuous agitation. Sample characterizations were performed by scanning electron microscopy, profilometry, contact angle measurement, X-ray diffraction, and X-ray photoelectron spectroscopy. The results showed that the samples exhibited a microporous structure with micro-roughness on surface, and the β -Ti phase was stabilized by complete niobium atoms diffusion in titanium matrix. In addition, the chemical treatment successfully modified the Ti-35Nb surface with micropore formation and enhancement of hydrophilic feature and TiO₂ and Nb₂O₅ layer, which can improve the biocompatibility of TiNb alloy implants.

Keywords: titanium-niobium alloy, powder metallurgy, controlled chemical oxidation, biomaterial.

1. INTRODUCTION

Titanium (Ti) – Niobium (Nb) alloys have attracted much attention in recent times as promising materials for fabrication of bone implants not only because their non-toxicity, high corrosion resistance and beneficial mechanical properties, but also because of their high biocompatibility, i.e. improved cell adhesion and proliferation, particularly on their oxidized surfaces [1].

Researchers have demonstrated that titanium and titanium alloy implants with porous structure, which may consist of macropores (100-500 μ m) and micropores (< 20 μ m), can encourage osseointegration and prevent implantation failure by providing spaces for bone cells, vascular and bone tissue ingrowth to form mechanical interlocking [2-5]. Metal implants with or without controlled porosity have been successfully fabricated by powder metallurgy (PM), proving to be an advantageous technique for processing Ti-based parts at low temperature without undesirable reactions or contaminations [6, 7]. These implants may have their bioactivity improved by various surface modification techniques, such as physical and chemical methods, which can modify the surface properties on a range of scales. Further, it is recognized that material-host tissue interactions are principally governed by surface cues [8].

In fact, surface characteristics play a vital role to improve the service life of metal implants. In principle, engineers and scientists have been seeking diverse techniques to develop the biocompatibility and the corrosion behavior of metal implants, aiming to make them adapt to the implant environment better. Superior corrosion behavior, improved wear resistance, better osseointegration rate, high biocompatibility and enhanced aesthetics are most important features which can be attained through surface modification [9]. Some examples of surface modification techniques which can be employed to improve the properties of titanium-based surfaces are: physical and chemical vapor deposition, laser cladding, thermal and chemical oxidation, thermal spraying, plasma spray, ion implantation, micro-arc oxidation, sandblasting, electrochemical treatment, sol-gel, biomimetic processes, bioceramic or biopolymer coating deposition and others [6, 10-15].

Among the various surface modification techniques, the controlled chemical oxidation to create reproducible nanopatterns on Ti and Ti alloy surfaces has received attention. By immersing the Ti-based materials, e.g. β -Ti alloys, in an etching solution made by mixing concentrated sulfuric acid (H_2SO_4 , a strong acid) and aqueous hydrogen peroxide (H_2O_2 , an oxidant), it is possible to create a reproducible network of nanopore on surface and generate a controlled surface roughness [8, 16, 17].

Based on the literature review, the controlled chemical oxidation successfully modified Ti and Ti alloy surfaces at the nanoscale for improving their bioactivity, but it lacks reports about the use of this technique for inducing modifications at the microscale. In this context, the present work aimed to investigate the ability of H_2SO_4/H_2O_2 solution to also create micropores on Ti-35Nb (wt%) substrates processed by powder metallurgy and enhance the oxide layer.

2. MATERIALS AND METHODS

2.1 Processing of Ti-35Nb substrates

Ti-35Nb (wt%) substrates were processed by powder metallurgy using Ti grade 2 powder (ASTM F67-00) manufactured by Baoji First Titanium Industry Co., and Nb grade 2 powder (ASTM B392-09e1) from the Brazilian Metallurgy and Mining Company (CBMM). The particle sizes of Ti ($< 53 \mu m$) and Nb ($< 62 \mu m$) powders were obtained by sieving.

Elemental powders of titanium grade 2 with 99.5% purity and niobium with 99.8% purity were mixed in the composition of Ti-65 wt.% and Nb-35 wt.%. The mechanical mixtures were conducted in a RetschTM MM 400 Mixer Mill for 15 min. at a vibrational frequency of $15 s^{-1}$. Then, the powder mixtures were uniaxially cold pressed at 730 MPa and sintered in a vacuum furnace (better than 10^{-5} Torr) for 2 hours at $1300^\circ C$ with heating rate of $10^\circ C/min$. Further, all substrates were cleaned by a sequence of ultrasonic bath, in order to eliminate the superficial organic impurities, and air-dried in an oven for 1 hour at $60^\circ C$. Such processing parameters were based on previous works [7, 18]

2.2 Controlled chemical oxidation of Ti-35Nb substrates

The cleaned Ti-35Nb substrates were submitted to the controlled chemical oxidation treatment with a mixture consisting of equal volumes of concentrated H_2SO_4 and 30% aqueous H_2O_2 for 4 hours (Ti-35Nb_4h) at room temperature under continuous agitation, according to literature data [8, 11, 17]. Later, the samples were rinsed with deionized water in an ultrasonic bath for 10 minutes and air-dried in an oven for 1 hour at $60^\circ C$. Before immersion of samples in the oxidative mixture, the components were mixed in an ice bath to control the exotherm of mixing and the cooling bath was removed to allow the temperature to rise to room temperature.

2.3 Characterization of Ti-35Nb samples

The microstructure of untreated Ti-35Nb sample (Ti-35Nb_Control) was analyzed by Scanning Electron Microscopy (SEM) conducted in FEI (model Inspect S) microscopy, operated at 20 kV. From images with magnification of 500 times, the pore size was measured by the calibrated scale bar from the image software of FEI Inspect S SEM. At the same magnification, the average porosity was determined by quantitative SEM image analysis, using ImageJ free software (version 1.52a), in about 37 random images.

Surface topography characterization of Ti-35Nb_Control and Ti-35Nb_4h samples was performed by Field Emission Scanning Electron Microscopy (FEG-SEM) conducted in a FEI (model Quanta FEG 450) microscopy, operated at 20 or 30 kV.

Surface roughness from Ti-35Nb_Control and Ti-35Nb_4h samples was evaluated by profilometry, using Nano Eva ST400 Z profilometer. The roughness profile parameters were assessed in three different regions of the same image for each sample, in order to determine the average roughness (Ra).

The wettability characteristics of control and treated surfaces were analyzed by distilled water contact angle measurements, using a contact angle meter (PocketGoniometer PGX+). This goniometer is equipped with a software capable of automatically measuring the contact angle (θ) in static mode on a sessile drop profile. To establish the balance of the involved forces, the contact angle was recorded 10 seconds after deposition of the drop on the surface of samples under ambient conditions. Each θ value corresponds to the average of 10 measurements.

Ti-35Nb_Control and Ti-35Nb_4h samples were characterized by X-ray Diffraction (XRD), using a Panalytical diffractometer (Model X'Pert Pro). The XRD equipment with CuK α ($\lambda = 1.54 \text{ \AA}$) monochro-

matic radiation was operated at 40 mA and 40 kV. The diffraction data were recorded in the 2θ interval from 5° to 80° with step size of 0.05° and count time of 2 s.

The chemical composition of control and treated surfaces was analyzed by X-ray Photoelectron Spectroscopy (XPS) using a Hemispherical Energy Analyzer (Specs Phoibos 150), equipped with an $AlK\alpha$ (1486.6 eV) unmonochromatic source at base pressures less than 10^{-10} mbar. All high-resolution spectra were charge-compensated by setting the binding energy of the C1s peak to 284.6 eV. Spectra were Shirley background-subtracted across the energy region and fitted using CasaXPS Version 2.3.14 (Casa Software Ltd., Cheshire, UK).

3. RESULTS AND DISCUSSION

3.1 Scanning Electron Microscopy (SEM)

Figure 1 shows the SEM image of Ti-35Nb_Control sample, where it is observed a microstructure composed of closed and homogeneously dispersed micropores with average size of $18.51 \pm 3.52 \mu\text{m}$, and the presence of Ti/Nb inter-particle necks. In addition, the result of quantitative image analyses indicated an average porosity of $1.37 \pm 0.47\%$. Such closed micropores and necks are intrinsic to the sintering process, which indicate that the sintering parameters were suitable to provide a satisfactory consolidation of Ti and Nb particles. Initially, the bonds develop mainly by atomic diffusion between adjacent particles, forming the neck region with a high degree of cohesion. As the temperature increases, the bonding surfaces increase, noting the inter-particle neck growth. Then, the intercommunicating pores are closed and simultaneously the closed pores are rounded off. Finally, in the last stage of sintering the coalescence and growth of the remaining pores occur. This stage consists of the contraction and elimination of the small and isolated pores and the growth of the larger pores, contributing to the free energy reduction of the system [19, 20].

Although closed-pore metal parts do not allow for much bone ingrowth, due to the large numbers of isolated pores, they still possess the potential to be used in orthopaedic load bearing implants. In particular, the lowered structural stiffness brought about by the presence of voids allows the reduction of their bulk stiffness, enabling a match with the mechanical properties of bone, which in turn reduces stress shielding of the bone host. This characteristic can be further enhanced by the low elastic moduli inherent to Ti-Nb alloys [21]. Thereby, the pore size, shape and distribution are of importance only because of the mechanical strength and fatigue resistance of the porous metal that is associated with these parameters. It has been stipulated that non-homogeneous distributions of pores as well as localized thin pore walls can lead to a reduced materials strength and early fatigue failure. Then, the fixation of implants based on closed-pore porous metal would have to be achieved by allowing bone ingrowth onto an additionally fabricated porous surface [22].

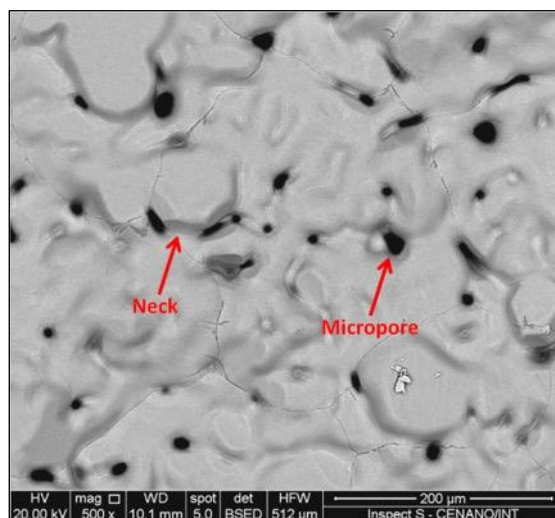


Figure 1: SEM image of Ti-35Nb_Control sample.

3.2 Field Emission Scanning Electron Microscopy (FEG-SEM)

Figure 2 exhibits FEG-SEM images and EDS spectra of untreated (Figures 2a and 2c) and treated (Figures 2b and 2d) samples. The surface with micro-roughness of the Ti-35Nb_Control sample can be seen in Figure 2(a). From Figure 2(b), it is noted that the simple combination of a concentrated acid and an oxidant agent was able to modify the Ti-35Nb surface, leading to formation of a microstructure composed of closed and open micropores with average size of $0.84 \pm 0.50 \mu\text{m}$ and angular shape, uniformly distributed across the surface. In addition, EDS spectra, Figures 2(c) and 2(d), revealed Ti, Nb, O and C peaks for all samples, suggesting no relevant chemical modification on the treated surface at micrometre scale.

According to literature, microporosity ($< 10 \mu\text{m}$) results in larger surface area that is believed to contribute to higher bone protein adsorption as well as to ion exchange and bone-like apatite formation by dissolution and reprecipitation, favoring cellular adhesion and implant osseointegration. Further, porous-surfaced implant provide a more effective means of dissipating implant forces over a greater volume of bone as a result of the three-dimensional bone-implant interlock. This allows the transfer of tensile, shear, and compressive forces from implant to bone, yielding greater mechanical stability at this critical interface [23, 25].

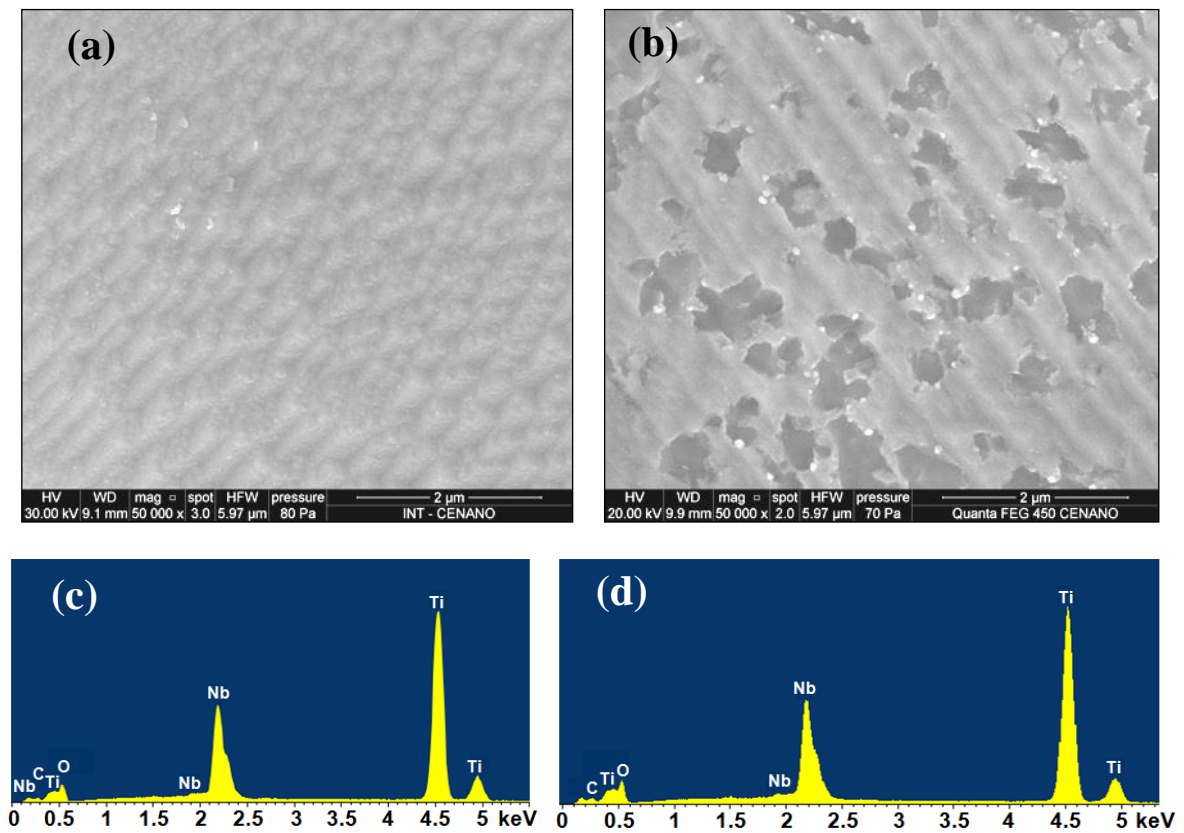


Figure 2: FEG-SEM images and EDS spectra: (a,c) Ti-35Nb_Control and (b,d) Ti-35Nb_4h.

3.3 Profilometry

The average roughness (R_a) of untreated and treated Ti-35Nb surfaces was obtained by profilometry. The roughness profiles indicated R_a values of $0.55 \pm 0.07 \mu\text{m}$ and $1.0 \pm 0.09 \mu\text{m}$ for Ti-35Nb_Control and Ti-35Nb_4h samples, respectively, demonstrating that the controlled chemical oxidation treatment was able to induce an increase in average roughness of Ti-35Nb surface. Moreover, the low standard deviations denote a uniform surface for both samples.

Such increase in roughness can enhance the bioactivity characteristics of metal implant surfaces, since some reports have shown that both the early fixation and long-term mechanical stability of the prosthesis can be improved by roughness profile in the range of 1-10 μm compared to smooth surfaces. For example, implant surfaces with micro-topographies, obtained from chemical treatments, have presented greater percentage of bone-to-implant contact when compared with machined or polished titanium-based surfaces [26, 27].

3.4 Contact angle measurement

Contact angle (θ) equal to 0° is an extreme situation of chemical affinity between surface and liquid and, therefore, the liquid material spreads completely on the solid surface (superhydrophilic surface). Contact angle equal to 180° is another extreme situation, where the liquid material presents no interaction with the solid surface (superhydrophobic surface). When θ is lower than 90° it is considered the surface is wet by liquid (hydrophilic surface). Otherwise, when θ is higher than 90° it is considered the surface is not wet by liquid (hydrophobic surface) [28].

Ti-35Nb_Control and Ti-35Nb_4h samples displayed average θ values of $50.4 \pm 1.5^\circ$ and $43.2 \pm 1.6^\circ$, respectively. It is observed that the controlled chemical oxidation treatment enhanced the hydrophilic feature of treated sample. This behavior is influenced by the surface topography of sample, which determines its hydrophilic or hydrophobic nature. For implant materials, a hydrophilic surface is considered to be desirable in view of its better interaction with biological fluids, cells and tissues [29, 30].

3.5 X-ray Diffraction (XRD)

Figure 3 presents the X-ray diffractograms: (a) Ti-35Nb_Control, and (b) Ti-35Nb_4h. The crystalline phases were identified according to X-ray powder diffraction patterns (PDF n° 01-089-4913). From Figures 3(a) and 3(b), the successful β -Ti phase stabilization is noted, suggesting that the processing parameters were suitable to form Ti-35Nb alloy with complete niobium atoms diffusion in titanium matrix. The sintering variables that can affect the alloy formation, such as temperature, time and atmosphere, require strict control [20]. In addition, titanium or niobium oxide peaks were not identified in both samples, which indicates that the oxide layer is very thin.

Studies have demonstrated that β -Ti alloys present superior properties compared to cp-Ti and Ti6Al4V, since their body-centered cubic microstructure causes an improved workability and remarkably lower elastic moduli, reducing the stress shielding effects. Moreover, β -stabilizing elements like, Nb, Ta, Zr, Mo or Sn have low cytotoxicity, which at the same time cause a high corrosion resistance related with very low metal release rates. This implies significantly improved tissue reactions and longevity of the implant material [17, 21, 31].

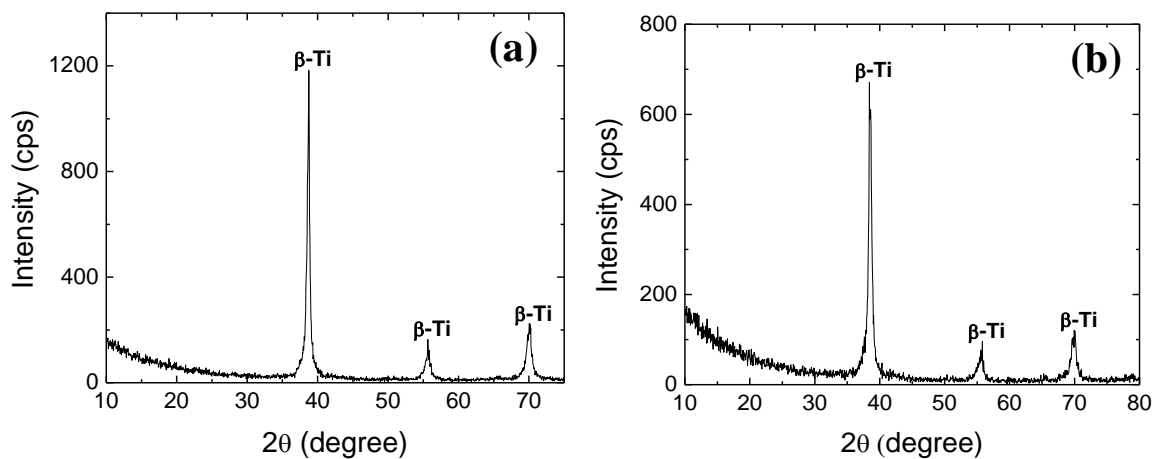


Figure 3: XRD diffractograms of the samples: (a) Ti-35Nb_Control and (b) Ti-35Nb_4h.

3.6 X-ray Photoelectron Spectroscopy (XPS)

High-resolution spectra of the Ti_{2p} , Nb_{3d} and O_{1s} core levels are displayed in Figure 4 for Ti-35Nb_Control (Figures 4a, 4b, 4c) and Ti-35Nb_4h (Figures 4d, 4e, 4f) samples. From Figures 4a (peaks at 458.3 eV and 463.9 eV) and 4d (peaks at 457.8 eV and 463.5 eV), it is noticed an intense Ti^{4+} doublet for both samples, demonstrating that TiO_2 is the main constituent of the oxide layer on surfaces. However, the deconvolution of Ti_{2p} peak suggested the occurrence of specie ascribed to Ti^{3+} like in Ti_2O_3 (Figure 4a: peaks at 456.4 eV and 461.4 eV; Figure 4b: peaks at 456.1 eV and 461.1 eV). Moreover, peaks at 453.9 eV and 460.1 eV (Figure 4a), and 453.6 eV and 459.7 eV (Figure 4d) are assigned to the $Ti^{metallic}$ [17]. This peak was considered to be from the Ti-35Nb substrates, since the native oxide layer is very thin [11]. But, a comparison between Figures 4a and 4d, it is noted that the $Ti^{metallic}$ peak completely disappeared for treated sample (Figure 4d), denot-

ing a significant modification of the Ti-35Nb surface by the controlled chemical oxidation treatment, which seems to have promoted a thickness increase of the TiO₂ layer.

From the Nb_{3d} core level spectra, in Figure 4b, the untreated sample presented a doublet at 203.7 eV and 206.2 eV attributed to Nb⁴⁺ (NbO₂). In the other hand, in Figure 4e, Ti-35Nb_4h sample showed a doublet at 206.8 eV and 209.5 eV related with Nb⁵⁺, indicating an effective oxidation of Ti-35Nb surface by H₂SO₄/H₂O₂ solution with layer growth of Nb₂O₅, assigned to the better resolution of Nb_{3d} spectrum in Figure 4e [17]. Further, Nb^{metallic} peak was not observed for both samples. This phenomenon may be related to the sintering process, which even performed under high vacuum, the residual oxygen presents in the furnace chamber can induce a thermal oxidation of surface.

The O_{1s} core level spectra are exhibited in Figures 4c (peak at 529.1 eV) and 4f (peak at 529.1 eV), which clearly indicate the O_{1s} peak from Ti-O or Nb-O bonds with shoulder peaks at higher energy for both samples. The deconvolution of O_{1s} spectra suggested that the origin of these shoulder peaks is due to oxygen in OH⁻ species (Figure 4c: peak at 531.8 eV; Figure 4f: peak at 530.3 eV) and adsorbed water (Figure 4c: peak at 533.7 eV; Figure 4f: peak at 531.9 eV). For Ti-35Nb_4h sample, in Figure 4f, the chemical treatment enhanced the O²⁻ peak relative to the shoulder, which can be related to the thickness growth of the oxide layer. The thickness increase of titanium and niobium oxide layer has a positive effect on the biocompatibility and kinetics of the bone formation process, since it avoid or reduce the diffusion of Ti and Nb ions from the bulk metal [32, 33]. Additionally, the OH⁻ content on the surface may improve the apatite nucleation and protein adsorption, since it give a negative charge to the oxide layer [34, 35].

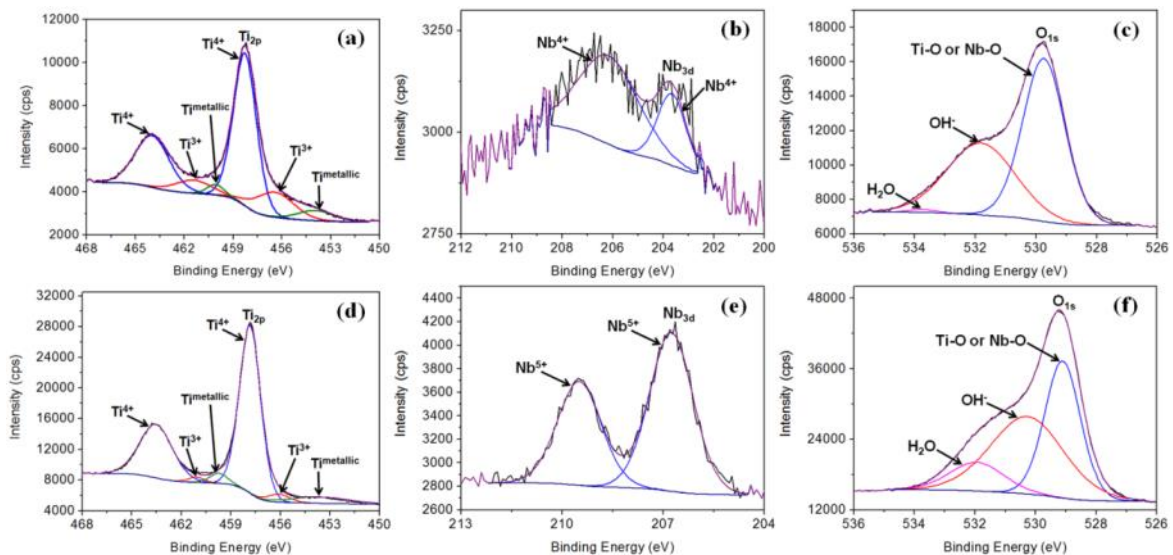


Figure 4: XPS spectra of the Ti_{2p}, Nb_{3d} and O_{1s} core levels for Ti-35Nb_Control (a,c,e) and Ti-35Nb_4h (b,d,f) samples.

4. CONCLUSIONS

Powder metallurgy technique successfully processed microporous Ti-35Nb samples with micro-roughness on surface, and stabilized β -Ti phase by complete niobium atoms diffusion in titanium matrix. H₂SO₄/H₂O₂ solution was able to generate micropores on the Ti-35Nb surface with $0.84 \pm 0.50 \mu\text{m}$ average size, enhancing the hydrophilic feature and oxide layer. In addition, the treated sample presented an oxide layer consisting predominantly of TiO₂ and Nb₂O₅ with negative charge provided by the presence of hydroxyl groups. Therefore, the results demonstrated that the used acid-oxidizing solution has also potential to modify TiNb alloy surfaces at the microscale.

5. ACKNOWLEDGMENTS

The authors thank to National Council for Scientific and Technological Development (CNPq/Brazil) for financial support.

6. BIBLIOGRAPHY

[1] VANDROVCOVA, M., JIRKA, I., NOVOTNA, K., *et al.*, "Interaction of human osteoblast-like Saos-2

- and MG-63 cells with thermally oxidized surfaces of a titanium-niobium alloy”, *PLoS One*, v. 9, n. 6, pp. 1-15, Jun. 2014.
- [2] VETRONE, F., VARIOLA, F., OLIVEIRA, P.T., *et al.*, “Nanoscale oxidative patterning of metallic surfaces to modulate cell activity and fate”, *Nano Letters*, v. 9, n. 2, pp. 659-665, Jan. 2009.
- [3] PUCKETT, S.D., LEE, P.P., CIOMBOR, D.M., *et al.*, “Nanotextured titanium surfaces for enhancing skin growth on transcutaneous osseointegrated devices”, *Acta Biomaterialia*, v. 6, n. 6, pp. 2352-2362, Jun. 2010.
- [4] PRADO, R.F., ESTEVES, G.C., SANTOS, E.L.S., *et al.*, “*In vitro* and *in vivo* biological performance of porous Ti alloys prepared by powder metallurgy”, *PLoS One*, v. 13, n. 5, pp. 1-22, May 2018.
- [5] XU, J., WENG, X.-J., WANG, X., *et al.*, “Potential use of porous titanium–niobium alloy in orthopedic implants: preparation and experimental study of its biocompatibility *in vitro*”, *PLoS One*, v. 8, n. 11, pp. e79289, Nov. 2013.
- [6] RIBEIRO, A.A., BALESTRA, R.M., ROCHA, M.N., *et al.*, “Dense and porous titanium substrates with biomimetic calcium phosphate coating”, *Applied Surface Science*, v. 265, pp. 250-256, Jan. 2013.
- [7] OLIVEIRA, C.S.S., GRIZA, S., OLIVEIRA, M.V., *et al.*, “Study of the porous Ti³⁵Nb alloy processing parameters for implant applications”, *Powder Technology*, v. 281, pp. 91-98, Sept. 2015.
- [8] VARIOLA, F., BRUNSKI, J.B., ORSINI, G., *et al.*, “Nanoscale surface modifications of medically relevant metals: state-of-the art and perspectives”, *Nanoscale*, v. 3, n. 2, pp. 335-353, Oct. 2010.
- [9] MOHAMMED, M.T., KHAN, Z.A., SIDDIQUEE, A.N., “Surface modifications of titanium materials for developing corrosion behavior in human body environment: a review”, *Procedia Materials Science*, v. 6, pp. 1610-1618, Sept. 2014.
- [10] RIBEIRO, A.A., MARQUES, R.F.C., GUASTALDI, A.C., *et al.*, “Hydroxyapatite deposition study through polymeric process on commercially pure Ti surfaces modified by laser beam irradiation”, *Journal of Materials Science*, v. 44, n. 15, pp.4056-4061, Aug. 2009.
- [11] YI, JI-H., BERNARD, C., VARIOLA, F., *et al.*, “Characterization of a bioactive nanotextured surface created by controlled chemical oxidation of titanium”, *Surface Science*, v. 600, n. 19, pp. 4613-4621, Oct. 2006.
- [12] RIBEIRO, A.A., VAZ, L.G., GUASTALDI, A.C., *et al.*, “Adhesion strength characterization of PVDF/HA coating on cp Ti surface modified by laser beam irradiation”, *Applied Surface Science*, v. 258, n. 24, pp. 10110–10114, Oct. 2012.
- [13] YILMAZ, E., GÖKÇE, A., FINDIK, F., *et al.*, “Metallurgical properties and biomimetic HA deposition performance of Ti-Nb PIM alloys”, *Journal of Alloys and Compounds*, v. 746, pp. 301-313, May 2018.
- [14] XIONG, J., LI, Y., HODGSON, P.D., *et al.*, “Nanohydroxyapatite coating on a titanium–niobium alloy by a hydrothermal process”, *Acta Biomaterialia*, v. 6, n. 4, pp. 1584-1590, Apr. 2010.
- [15] MEDDA, R., HELTH, A., HERRE, P., *et al.*, “Investigation of early cell–surface interactions of human mesenchymal stem cells on nanopatterned β -type titanium–niobium alloy surfaces”, *Interface Focus*, v. 4, n. 1, pp. 1-10, Feb. 2014.
- [16] GOSTIN, P.F., HELTH, A., VOSS, A., *et al.*, “Surface treatment, corrosion behavior and apatite-forming ability of Ti-45Nb implant alloy”, *Journal of Biomedical Materials Research, Part B: Applied Biomaterials*, v. 101, n. 2, pp. 269-278, Feb. 2013.
- [17] HELTH, A., GOSTIN, P.F., OSWALD, S., *et al.*, “Chemical nanoroughening of Ti40Nb surfaces and its effect on human mesenchymal stromal cell response”, *Journal of Biomedical Materials Research, Part B: Applied Biomaterials*, v. 102, n. 1, pp. 31-41, Jan. 2014.
- [18] DE BLAS, J.G., LUNZ, J.N., GUZELA, L.R., *et al.*, “Avaliação da homogeneização de liga Ti35Nb processada por metalurgia do pó e extrusão angular em canal”, In: *Anais do 71º Congresso Anual da ABM*, pp. 635-642, Rio de Janeiro, Set. 2016.
- [19] RIBEIRO, A.A., MORANI, L.M., BALESTRA, R.M., *et al.*, “Study of sol-gel/powder metallurgy technique for processing titanium parts”, *Materials Science Forum*, v. 727-728, pp. 368-373, Aug. 2012.
- [20] CREMONEZI, A., KLEIN, A.N., LOBERTO, A., *et al.*, *A metalurgia do pó: alternativa econômica com menor impacto ambiental*, 1ª Ed., São Paulo, Grupo Setorial de Metalurgia do Pó, 2009.
- [21] ROSENBERG, R., STAROSVETSKY, D., GOTMAN, I., “Surface modification of a low modulus Ti-Nb alloy for use in medical implants”, *Journal of Materials Science Letters*, v. 22, n. 1, pp. 29-32, Jan. 2003.

- [22] RYAN, G., PANDIT, A., APATSIDIS, D.P., “Fabrication methods of porous metals for use in orthopaedic applications”, *Biomaterials*, v. 27, n. 13, pp. 2651-2670, May 2006.
- [23] KARAGEORGIU, V., KAPLAN, D., “Porosity of 3D biomaterial scaffolds and osteogenesis”, *Biomaterials*, v. 26, n. 27, pp. 5474-5492, Sept. 2005.
- [24] PILLIAR, R.M. “Implant surface design for development and maintenance of osseointegration”, In: ELLINGSEN, J.E., LYGSTADAAS, S.P. (eds), *Bio-implant interface: improving biomaterials and tissue reactions*, chapter 3, Boca Raton, USA, CRC Press LLC, 2003.
- [25] LE GUÉHENNEC, L., SOUEIDAN, A., LAYROLLE, P., *et al.*, “Surface treatments of titanium dental implants for rapid osseointegration”, *Dental Materials*, v. 23, n. 7, pp. 844-854, Jul. 2007.
- [26] CHRCANOVIC, B.R., MARTINS, M.D., “Study of the influence of acid etching treatments on the superficial characteristics of Ti”, *Materials Research*, v. 17, n. 2, pp. 373-380, Apr. 2014.
- [27] ALLA, R.K., GINJUPALLI, K., UPADHYA, N., *et al.*, “Surface roughness of implants: a review”, *Trends in Biomaterials and Artificial Organs*, v. 25, n. 3, pp. 112-118, May 2011.
- [28] LIM, Y., OSHIDA, Y., “Initial contact angle measurements on variously treated dental/medical titanium materials”, *Bio-Medical Materials and Engineering*, v. 11, n. 4, pp. 325-341, Feb. 2001.
- [29] STRNAD, G., CHIRILIA, N., PETROVAN, C., *et al.*, “Contact angle measurement on medical implant titanium based biomaterials”, *Procedia Technology*, v. 22, pp. 946-953, Dec. 2016.
- [30] JAMESH, M., NARAYANAN, T., CHU, P., *et al.*, “Effect of surface mechanical attrition treatment of titanium using alumina balls: surface roughness, contact angle and apatite forming ability”, *Frontiers of Materials Science*, v. 7, n. 3, pp. 285-294, Sept. 2013.
- [31] TORRES-SANCHEZ, C., MCLAUGHLIN, J., BONALLO, R., “Effect of pore size, morphology and orientation on the bulk Stiffness of a porous Ti35Nb4Sn alloy”, *Journal of Materials Engineering and Performance*, v. 27, n. 6, pp. 2899-2909, Jun. 2018.
- [32] CASALETTO, M.P., INGO, G.M., KACILIUS, S., *et al.*, “Surface studies of in vitro biocompatibility of titanium oxide coatings”, *Applied Surface Science*, v. 172, n. 1-2, pp. 167-177, Mar. 2001.
- [33] WANG, G., LI, J., LV, K., *et al.*, “Surface thermal oxidation on titanium implants to enhance osteogenic activity and *in vivo* osseointegration”, *Scientific Reports*, v. 6, n. 31769, pp. 1-13, Aug. 2016.
- [34] CHEN, X., NOURI, A., LI, Y., *et al.*, “Effect of surface roughness of Ti, Zr, and TiZr on apatite precipitation from simulated body fluid”, *Biotechnology and Bioengineering*, v. 101, n. 2, pp. 378-387, Oct. 2008.
- [35] WANG, X., HAYAKAWA, S., TSURU, K., *et al.*, “Bioactive titania gel layers formed by chemical treatment of Ti substrate with a H₂O₂/HCl solution”, *Biomaterials*, v. 23, n. 5, pp. 1353-1357, Mar. 2002.

ORCID

Alexandre Antunes Ribeiro
Rodrigo Sacramento da Silva

<https://orcid.org/0000-0002-5299-4241>
<https://orcid.org/0000-0002-6465-9248>